[17] W. Nishida, Y. Kitami, K. Hiwada, cDNA cloning and mRNA expression of calponin and SM22 in rat aorta smooth muscle cells, Gene 130 (1993) 297–302.
[18] L. Li, J.M. Miano, P. Cserjesi, E.N. Olson, SM22α, a marker of adult smooth muscle, is expressed in multiple myogenic lineages during embryogenesis, Circ. Res. 78 (1996) 188–195.
[19] T.N. Sato, Y. Qin, C.A. Kozak, K.L. Audus, Tie-1 and tie-2 define another class of putative receptor tyrosine kinase genes expressed in early embryonic vascular system, Proc. Natl. Acad. Sci. USA 90 (1993) 9355–9358.
[20] S. Davis, T.H. Aldrich, P.F. Jones, A. Acheson, D.L. Compton, V. Jain, T.E. Ryan, J. Bruno, C. Radziejewski, P.C. Maisonpierre, G.D. Yancopoulous, Isolation of angiopoietin-1, a ligand for the TIE2 receptor, by secretion-trap expressing cloning, Cell 87 (1996) 1161–1169.
[21] H. Schnürch, W. Risau, Expression of tie-2, a member of a novel family of receptor tyrosine kinases, in the endothelial cell lineage, Development 119 (1993) 957–968.
[22] A.L. Wong, Z.A. Haroon, S. Werner, M.W. Dewhirst, C.S. Greenberg, K.G. Peters, Tie2 expression and phosphorylation in angiogenic and quiescent adult tissues, Circ. Res. 81 (1997) 567–574.
[23] Y. Shirakata, R. Kimura, D. Nanba, R. Iwamoto, S. Tokumaru, C. Morimoto, K. Yokota, M. Nakamura, K. Sayama, E. Mekada, S. Higashiyama, K. Hashimoto, Heparin-binding EGF-like growth factor accelerates keratinocyte migration and skin wound healing, J. Cell Sci. 118 (2005) 2363–2370.
[24] L. Li, J.M. Miano, M. Mercer, E.N. Olson, Expression of the *SM22α* promoter in transgenic mice provides evidence for distinct transcriptional regulatory programs in vascular and visceral smooth muscle cells, J. Cell Biol. 132 (1996) 849–859.
[25] Y. Nakajima, V. Mironov, T. Yamagishi, H. Nakamura, R.R. Markwald, Expression of smooth muscle alpha-actin in mesenchymal cells during formation of avian endocardial cushion tissue: a role for transforming growth factor β3, Dev. Dyn. 209 (1997) 296–309.
[26] F.J. de Lange, A.F.M. Moorman, R.H. Anderson, J. Männer, A.T. Soufan, C. de Gier-de Vries, M.D. Schneider, S. Webb, M.J.B. van den Hoff, V.M. Christoffels, Lineage and morphogenetic analysis of the cardiac valves, Cir. Res. 95 (2004) 645–654.
[27] S. Yamazaki, R. Iwamoto, K. Saeki, M. Asakura, S. Takashima, A. Yamazaki, R. Kimura, H. Mizushima, H. Moribe, S. Higashiyama, M. Endoh, Y. Kaneda, S. Takagi, S. Itami, N. Takeda, G. Yamada, E. Mekada, Mice with defects in HB-EGF ectodomain shedding show severe developmental abnormarities, J. Cell Biol. 163 (2003) 469–475.
[28] R. Iwamoto, E. Mekada, ErbB and HB-EGF signaling in heart development and function, Cell Struct. Funct. 31 (2006) 1–14.
[29] J. Lin, L. Hutchinson, S.M. Gaston, G. Raab, M.R. Freeman, BAG-1 is a novel cytoplasmic binding partner of the membrane form of heparin-binding EGF-like growth factor: a unique role for proHB-EGF in cell survival regulation, J. Biol. Chem. 276 (2001) 30127–30132.
[30] D. Nanba, A. Mammoto, K. Hashimoto, S. Higashiyama, Proteolytic release of the carboxy-terminal fragment of proHB-EGF causes nuclear export of PLZF, J. Cell Biol. 163 (2003) 489–502.
[31] X. Wang, H. Mizushima, S. Adachi, M. Ohishi, R. Iwamoto, E. Makada, Cytoplasmic domain phosphorylation of heparin-binding EGF-likegrowth factor, Cell Struct. Funct. 31 (2006) 15–27.

Oncogene (2007) 26, 339–348

www.nature.com/onc

ORIGINAL ARTICLE

Pre-B-cell leukemia transcription factor 1 is a major target of promyelocytic leukemia zinc-finger-mediated melanoma cell growth suppression

K Shiraishi[1,2], K Yamasaki[2], D Nanba[1], H Inoue[1], Y Hanakawa[2], Y Shirakata[2], K Hashimoto[2] and S Higashiyama[1,3]

[1]Department of Biochemistry and Molecular Genetics, Ehime University Graduate School of Medicine, Shitsukawa, Toon, Ehime, Japan; [2]Department of Dermatology, Ehime University Graduate School of Medicine, Shitsukawa, Toon, Ehime, Japan and [3]Precursory Research for Embryonic Science and Technology (PRESTO), Japan Science and Technology Corporation (JST), Kawaguchi City, Saitama, Japan

Promyelocytic leukemia zinc-finger (PLZF) is a transcriptional repressor and tumor suppressor. PLZF is expressed in melanocytes but not in melanoma cells, and recovery of PLZF expression markedly suppresses melanoma cell growth. Several target genes regulated by PLZF have been identified, but the precise function of PLZF remains uncertain. Here, we searched for candidate target genes of PLZF by DNA microarray analysis. Pre-B-cell leukemia transcription factor 1 (Pbx1) was one of the prominently suppressed genes. Pbx1 was highly expressed in melanoma cells, and its expression was reduced by transduction with the PLZF gene. Moreover, the growth suppression mediated by PLZF was reversed by enforced expression of Pbx1. Knockdown of Pbx1 by specific small interfering RNAs suppressed melanoma cell growth. We also found that Pbx1 binds HoxB7. Reverse transcription–polymerase chain reaction analysis demonstrated that repression of Pbx1 by PLZF reduces the expression of HoxB7 target genes, including tumor-associated neoangiogenesis factors such as basic fibroblast growth factor, angiopoietin-2 and matrix metalloprotease 9. These findings suggest that deregulation of Pbx1 expression owing to loss of PLZF expression contributes to the progression and/or pathogenesis of melanoma.
Oncogene (2007) **26**, 339–348. doi:10.1038/sj.onc.1209800; published online 24 July 2006

Keywords: Pbx1; PLZF; Hox; melanoma

Introduction

Malignant melanoma is a highly aggressive neoplastic disease whose incidence is increasing rapidly. To develop new therapies, it is essential to elucidate the molecular mechanisms by which melanocytes are transformed into malignant melanoma cells. A recent report found that the promyelocytic leukemia zinc-finger (PLZF) protein is expressed in melanocytes but not in melanoma cells, and that melanoma growth is markedly suppressed by enforced expression of PLZF (Felicetti *et al.*, 2004).

PLZF was first identified by its translocation with retinoic acid receptor alpha in t(11;17) acute promyelocytic leukemia (Chen *et al.*, 1993). The PLZF protein is a sequence-specific transcription repressor characterized by a BTB/POZ domain, which is responsible for transcriptional repression, and nine zinc-finger domains that form the DNA-binding domain (Hong *et al.*, 1997; Li *et al.*, 1997; Wong and Privalsky, 1998). Some target genes regulated by PLZF have been identified. Studies of PLZF-knockout mice indicate that PLZF represses HoxD gene expression through chromatin remodeling, which in turn regulates limb and axial skeletal patterning (Barna *et al.*, 2000, 2002). PLZF also binds to and represses the cyclin A2 promoter, and is involved in the regulation of cell cycle progression (Yeyati *et al.*, 1999). Moreover, PLZF represses c-*myc* expression, which is central to the control of cellular proliferation, apoptosis and differentiation (McConnell *et al.*, 2003). DNA microarray analyses have also revealed numerous candidate genes targeted by PLZF (McConnell *et al.*, 2003; Costoya *et al.*, 2004; Felicetti *et al.*, 2004). These target genes may have a great influence on the progression of melanoma, but their role in the aggressiveness of this cancer remains unknown.

For this reason, we used DNA microarray analysis to search for additional PLZF target genes. One of the most strongly regulated genes identified was pre-B-cell leukemia transcription factor 1 (Pbx1). Pbx1 is also a transcriptional regulator and a binding partner for a number of Hox proteins (Mann and Chan, 1996; Shanmugam *et al.*, 1997). We confirmed that Pbx1 is highly expressed in melanoma cells and that cell growth is markedly suppressed when its expression is knocked down. Furthermore, we identified HoxB7 as a binding

Correspondence: Dr S Higashiyama, Department of Biochemistry and Molecular Genetics, Ehime University Graduate School of Medicine, Shitsukawa, Toon, Ehime 791-0295, Japan.
E-mail: shigeki@m.ehime-u.ac.jp
Received 1 November 2005; revised 30 May 2006; accepted 31 May 2006; published online 24 July 2006

partner of Pbx1 in melanoma cells. We show here that PLZF suppresses the expression of Pbx1-HoxB7 target genes as well as Pbx1 itself and that dysregulation of this network owing to loss of PLZF may play an important role in the progression of melanoma.

Results

PLZF suppresses Pbx1 gene expression

Felicetti *et al.* (2004) reported that primary melanomas and melanoma cell lines completely lack PLZF gene expression and that enforced expression of PLZF in melanoma cell lines suppressed their growth *in vitro* and *in vivo*. We confirmed these results using 15 melanoma cell lines, including A375, 397 cell lines and their PLZF transfectants (data not shown).

We then examined which genes are repressed by PLZF in the melanoma cells by DNA microarray analysis. For these experiments, we constructed adenovirus vectors carrying the genes encoding PLZF and LacZ and used them to infect A375 and 397 cells at a multiplicity of infection (MOI) of 200. Several genes exhibited different levels of expression in PLZF-negative and PLZF-positive cells. We found that Pbx1 was the most prominently downregulated transcription factor in PLZF-positive cells (Table 1). Reverse transcription–polymerase chain reaction (RT–PCR) confirmed that Pbx1 mRNA expression in A375 cells was clearly and substantially reduced in a time-dependent manner after infection with the PLZF adenovirus (Figure 1a). The expression of Pbx1 mRNA decreased to 25% of that in LacZ-infected cells. In addition, the Pbx1 protein levels in the PLZF-infected cells decreased by approximately 40% when compared with cells infected with the LacZ adenovirus or non-infected cells (Figure 1b). We also obtained similar results in 397 cells.

Enforced expression of Pbx1 rescues growth suppression by PLZF

In order to determine the relative importance of PLZF-mediated downregulation of Pbx1 in the growth of melanoma cells, we examined the proliferation of stable PLZF-expressing melanoma cells transfected with the pME18S-Pbx1 or pME18S control vector. Pbx1 protein levels in the transfected cells were first estimated by Western blotting (Figure 2a). Pbx1 levels increased approximately 1.5- and 1.3-fold in A375P and A375 cells, respectively, in comparison with controls. We also examined transfection efficiency in these cells using the mixture of pME18S-Pbx1 and pME18S-ECFP (Enhanced Cyan Fluorescent Protein) vectors. We found that approximately 65% of the cells were CFP (Cyan Fluorescent Protein)-positive (Figure 2b, inset). We then investigated the growth of A375 and A375P cells after transient transfection with pME18S-Pbx1 or pME18S. Exogenous expression of Pbx1 did not cause further enhancement of A375 cell growth. This suggests that there was sufficient endogenous Pbx1 expression. A375P cells exhibited a marked downregulation of both endogenous Pbx1 expression and cell growth. This effect was partially (approximately 40%) rescued by the expression of exogenous Pbx1 (Figure 2b), thus suggesting the presence of a Pbx1-independent pathway in PLZF-transfected melanoma cells. We also obtained similar results in 397 and 397P cells (data not shown).

Table 1 Expression profile obtained by array hybridization

Genes[a]	*Description*	*Accession number*	*Ratio (PLF/LacZ)*	
tzfp	Testis zinc-finger protein	NM_014383	Up	> × 20
pnkp	Polynucleotide kinase 3′-phosphatase	NM_007254	Up	
mapk4	Mitogen-activated protein kinase 4	XM_008806	Up	
oas3	2′–5′ Oligoadenylate synthetase 3	NM_006187	Up	× 10– × 20
osmr	Oncostatin m receptor	NM_003999	Up	
fezl	Zygin I, isoform 1	NM 005103	Up	
tssc3	Tumor-suppressing subtransferable candidate 3	NM 003311	Up	
lmo6	Linn domain-only 6	NML006150	Up	
nfsl	Nfsl nitrogen fixation 1	NM_021100	Up	× 5– × 10
cir	Ebfl-interacting corepressor	NM_004882	Up	
btebl	Basic transcription element-binding protein 1	NM_001206	Up	
netl	P65 netl proto-oncogene protein	S82401	Down	< × 0.05
cacng7	Calcium channel gamma subunit 7	AF2S8387	Down	× 0.05– × 0.1
rgs6	Regulator of g-protein signalling 6	NM 004296	Down	
pbxl	Pre-B-cell leukemia transcription factor 1	NM_002585	Down	× 0.1– × 0.2
calbl	Calbindinl	NM_004929	Down	
arhgdig	rho gdp dissociation inhibitor gamma	NM_001176	Down	
chrna 10	Cholinergic receptor, alpha polypeptide 10	NM_020402	Down	
hgc6.2	Hgc6.2 protein	NM_014356	Down	
dc20	Dc20	AF311338	Down	
serpinhl	Serine proteinase inhibitor, clade h, member 1	NM_004353	Down	

Adenoviral transduction of PLZF was chosen for expressing PLZF in A375 and 397 cells instead of stably expressing of PLZF, because of (1) avoiding the bias of cell response for PLZF by cloning of drug-resistant cells and (2) controlling the expression level of PLZF. The levels of HoxB7, bFGF, Ang-2 and MMP9 were in the range of × 0.25– × 0.5. [a]These genes were common in both A375 and 397 cells in duplicate microarray analyses.

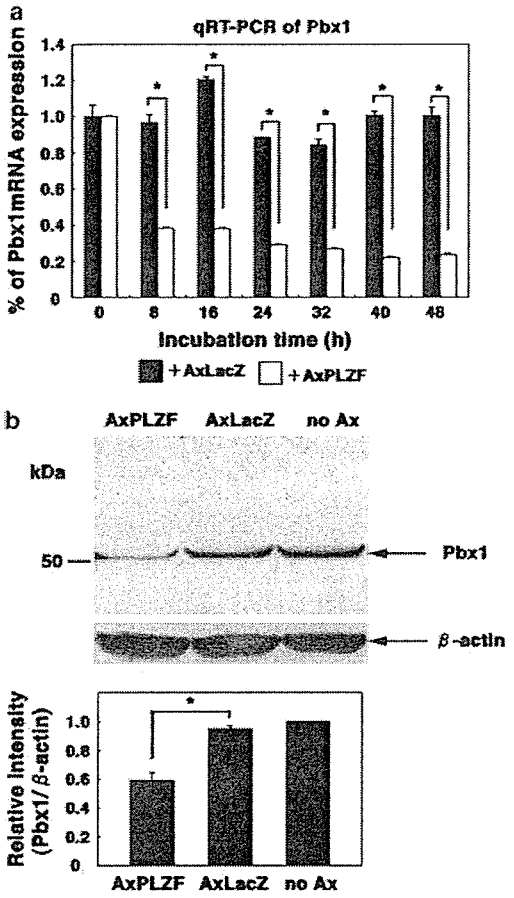

Figure 1 PLZF suppresses Pbx1 gene expression. (a) qRT–PCR of Pbx1 mRNA in A375 cells infected with LacZ or PLZF adenovirus. $^*P<0.05$. (b) Upper panel: Western blot analysis of Pbx1 protein in A375 cells infected with LacZ or PLZF adenovirus and in uninfected cells. Lower panel: Relative intensity of Pbx1 proteins calculated as a ratio vs expression of β-actin. $^*P<0.05$. AxLacZ, infection with LacZ adenovirus (MOI 200); AxPLZF, infection with PLZF adenovirus (MOI 200); no Ax, no infection. Each experiment was performed in duplicate.

PLZF physically interacts with the Pbx1 promoter

In order to demonstrate direct regulation of the Pbx1 gene by PLZF, we searched the Pbx1 promoter for a putative PLZF-binding site using the TFSEARCH program (Heinemeyer *et al*., 1998, http://mbs.cbrc.jp/research/db/TFSERCHJ.html), which suggested seven potential PLZF DNA recognition sequences located within a 3.0-kb region upstream of the transcription initiation site (Figure 3a). We then used a 3.0-kb fragment of the Pbx1 promoter in a reporter assay. The luciferase activity of Pbx1–3.0 was markedly suppressed in A375P, as compared to A375 cells (Figure 3b). Electrophoretic mobility shift assay (EMSA) was subsequently performed with nuclear extracts made from A375 cells infected with PLZF adenovirus and uninfected cells in order to identify the PLZF DNA recognition site in the Pbx1 promoter. Site 1 (2998 bp upstream) and Site 4 (2433 bp upstream) bound with factors in the A375 cell extracts without

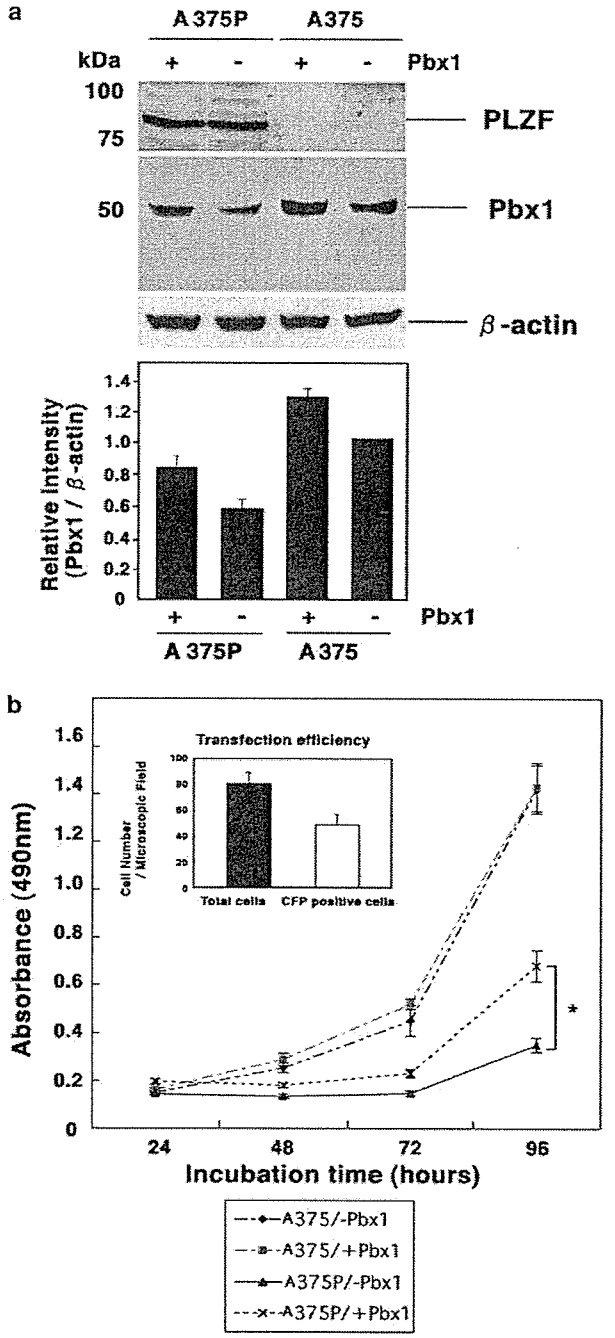

Figure 2 Enforced expression of Pbx1 rescues growth suppression of melanoma cells by PLZF. (a) Upper panel: Western blot analysis of PLZF and Pbx1 in A375 and A375P cells transfected with PME18S-Pbx1 or PME18S control vector. Lower panel: Relative intensity of Pbx1 protein, which was calculated as the ratio of Pbx1 vs β-actin. (b) Growth curves of A375 and A375P cells transfected with PME18S-Pbx1 and PME18S control vector. $^*P<0.05$. Inset: Transfection efficiency of pME18S-Pbx1 was evaluated by counting CFP-positive cells transfected with both PME18S-Pbx1 and pME18S-ECFP.

PLZF expression (stars in lane 1 and lane 7), and formed another complex in the A375 cell extracts expressing PLZF (arrow in lane 2, Figure 3c). On the other hand,

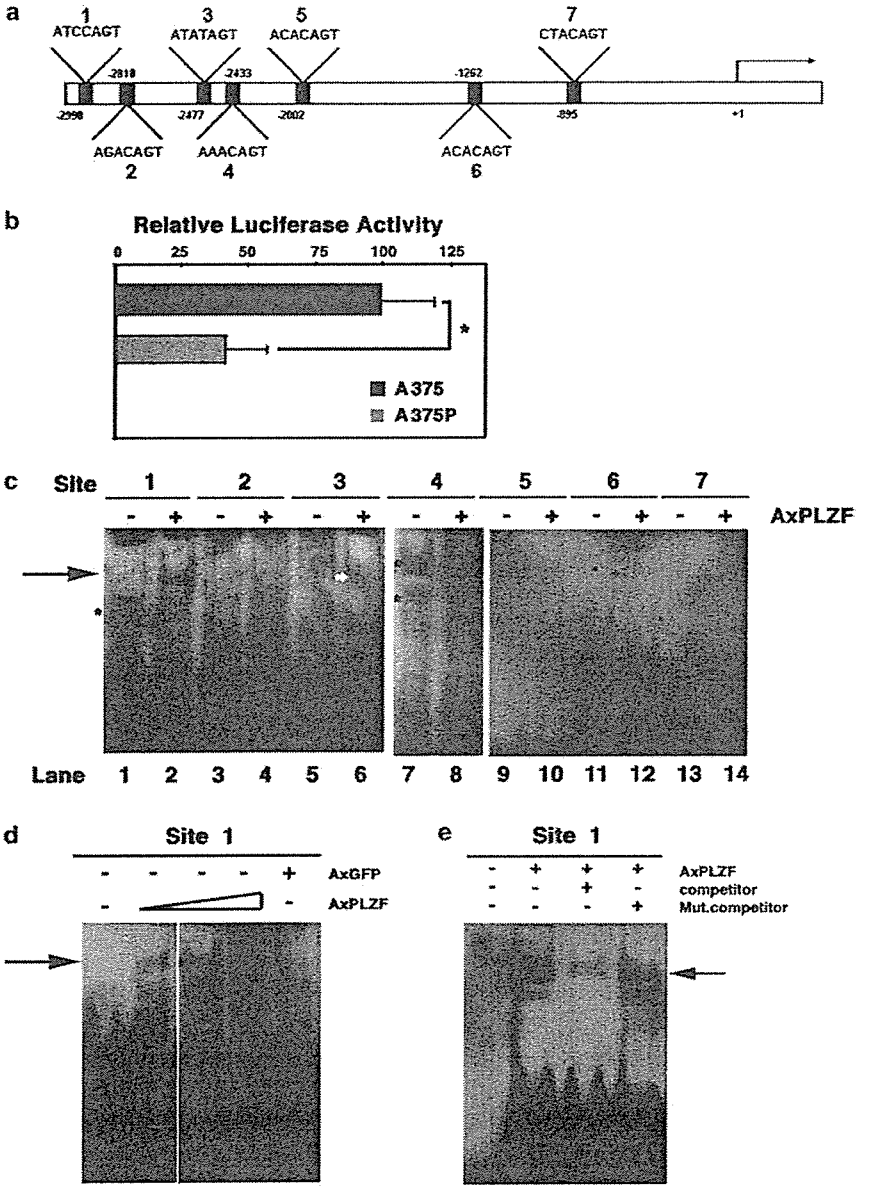

Figure 3 PLZF protein directly interacts with the Pbx1 promoter. (**a**) Schematic depiction of the Pbx1 promoter region and seven potential binding sites for PLZF (Sites 1–7). The +1 position corresponds to the initiation site of transcription. (**b**) Relative luciferase activity measured at 24 h after transfection of pGL Pbx1–3.0 into A375 cells and A375P cells. Each experiment was performed in triplicate and data represent the means ± s.d. of three independent experiments. (**c**) EMSA carried out with nuclear extracts of A375 cells infected with PLZF adenovirus (MOI 100) and uninfected cells. White arrowhead in lane 6 shows stain. (**d**) Specificity of interaction between PLZF and Site 1 (an arrow) was confirmed by EMSA using nuclear extracts of A375 cells infected with PLZF (MOI 50, 100 and 200) or GFP adenovirus (MOI 200). (**e**) Interaction between PLZF and Site 1 (an arrow) was found to compete with unlabeled Site 1 but not with unlabeled mut. Site 1.

Sites 2, 3, 4, 5, 6 and 7 did not form additional complexes in the A375 cell extracts expressing PLZF, as compared to A375 cell extracts without PLZF (lanes 3–14, see comments on lane 6 in figure legends). To confirm the specificity of the interaction between Site 1 and PLZF, we carried out dose–response analysis and competition analysis. The interaction between Site 1 and PLZF exhibited a dose-dependent relationship (Figure 3d), and was completely abolished by the addition of the competitor (unlabeled Site 1). The competitor with the mutation (mutated Site 1, see 'Materials and methods') failed to abolish the PLZF–Site 1 interaction (Figure 3e). On the other hand, deletion of Site 1 from Pbx1–3.0 (Pbx1–3.0/ΔSite 1) did not show significant recovery of Pbx1 promoter activity (data not shown), indicating that Site 1 is an interactive site for PLZF, and is not sufficient for complete repression of Pbx1 gene expression. These results

suggest that repression of Pbx1 gene expression by PLZF is regulated by multiply direct and/or indirect mechanisms.

Melanoma cell growth is suppressed by Pbx1 small interfering RNAs

In order to further characterize the role of Pbx1 in melanoma cell growth, we examined the suppression of melanoma cell growth by Pbx1 knockdown using two types of small interfering RNA (siRNA) (siRNA1 and siRNA2). Mutated siRNAs (mut. siRNA1 and mut. siRNA2) were used as controls. We confirmed that transfection of A375 and 397 cells with Pbx1 siRNA1 significantly reduced Pbx1 mRNA (data not shown) and protein levels (Figure 4a). In addition, transfection of A375 and 397 cells with Pbx1 siRNA1, but not Pbx1 mut. siRNA1, caused marked and statistically significant suppression of cell growth (Figure 4b). These data suggest that Pbx1 is involved in cell growth of A375 and 397 cells. siRNA2 showed similar results as siRNA1 (data not shown).

Pbx1 binds HoxB7

Pbx1 forms complexes with a number of Hox proteins, and HoxB7 was expressed strongly in all melanoma cell lines tested (Care *et al*., 1996). We investigated whether Pbx1 interacts with HoxB7 in A375 and 397 cells. HoxB7 was immunoprecipitated from cell lysates and was then analysed by immunoblotting with anti-Pbx1 antibody. We detected a 52-kDa band corresponding to Pbx1 in both cell lines (Figure 5). We also found that an anti-Pbx1 antibody co-immunoprecipitated HoxB7 from the same cell lysates (data not shown).

Expression of HoxB7 target genes is downregulated by reduction of Pbx1

We investigated the effects of Pbx1 knockdown on the expression of HoxB7 and its target genes. Knockdown

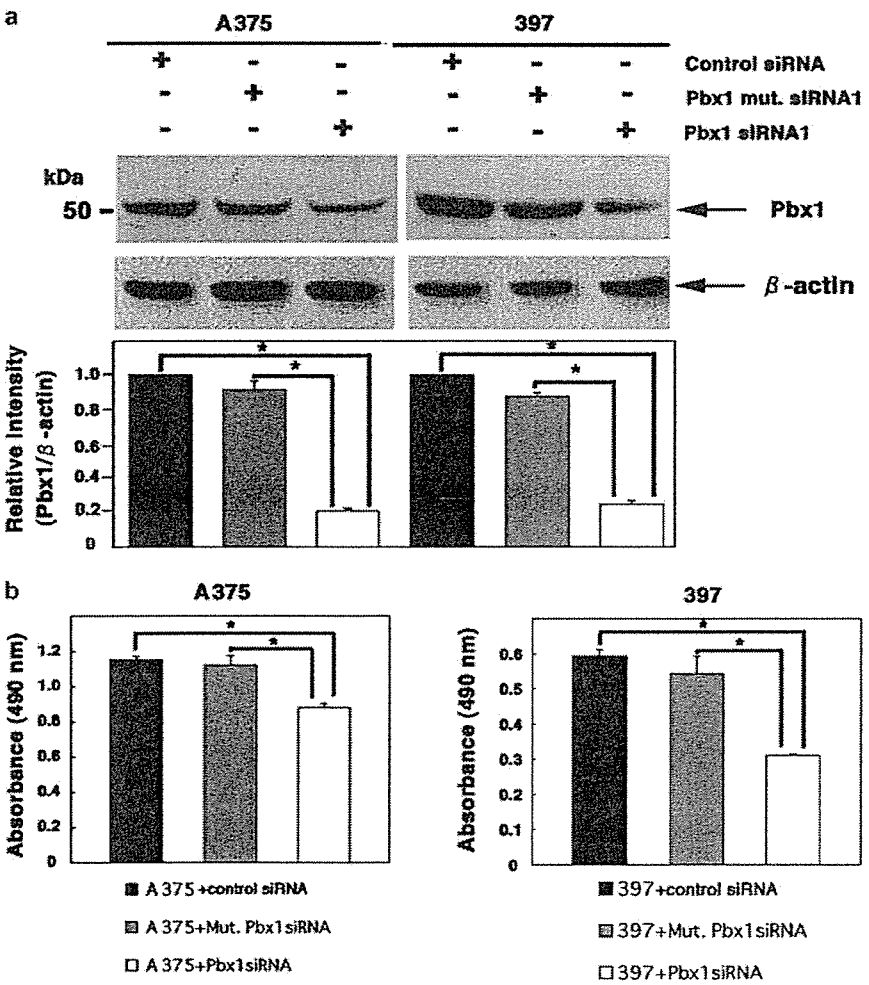

Figure 4 Melanoma cell growth is suppressed by Pbx1 siRNAs. (**a**) Upper panel: Western blot analysis of Pbx1 in control siRNA-, mutated-Pbx1 siRNA- and Pbx1 siRNA-transduced melanoma cells. Lower panel: Relative intensity of Pbx1 protein expression calculated as the ratio of Pbx1 vs β-actin. $*P<0.05$. (**b**) Cell proliferation of melanoma cells transfected with each siRNA. $*P<0.05$. Each experiment was performed in triplicate.

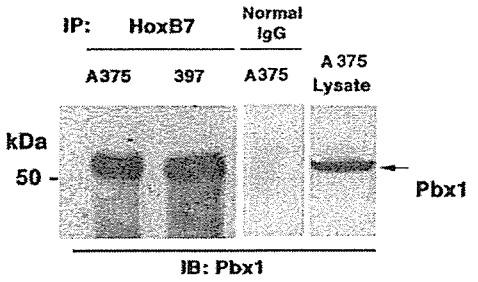

Figure 5 Pbx1 binds HoxB7. Interaction between Pbx1 and HoxB7 as assessed by immunoprecipitation. A375 and 397 cell lysates were immunoprecipitated with anti-HoxB7 antibody and immunoblotted with anti-Pbx1 antibody. Sodium dodecyl sulfate–polyacrylamide gel electrophoresis was carried out under the non-reducing condition.

of Pbx1 with the siRNAs slightly reduced the mRNA expression of HoxB7 (Figure 6a). It remains uncertain whether Pbx1 binds directly to the promoter region of the HoxB7 gene. HoxB7 is reported to regulate the expression of basic fibroblast growth factor (bFGF), angiopoietin-2 (Ang-2), matrix metalloprotease 9 (MMP9), growth-related oncogene-α (GROα), interleukin-8 (IL-8) and vascular endothelial growth factor (VEGF) (Care *et al.*, 1996, 2001). We thus evaluated the effects of Pbx1 knockdown on the expression of the target genes. As shown in Figure 6b, knockdown of Pbx1 markedly reduced the level of bFGF mRNA, and mildly did those of Ang-2 and MMP mRNAs, whereas those of GROα, IL-8 and VEGF were unchanged. Pbx1 knockdown significantly reduced protein levels of Ang-2 and MMP9, but it did not seem to have any effect on the protein levels of bFGF. This may be owing to the short culture duration and/or long half-life of bFGF protein. We obtained similar results in 397 cells (data not shown).

We further examined whether enforced expression of PLZF in melanoma cells would reduce HoxB7, bFGF, Ang-2 and MMP9. Quantitative RT–PCR analysis revealed that transcripts of all of these were significantly reduced in both A375P and 397P cells (Figure 7). These data suggest that the PLZF–Pbx1 axis is important in regulating HoxB7 target genes via Pbx1/HoxB7 heterocomplex formation.

Discussion

In this study, we performed DNA microarray analysis and found that Pbx1 is a prominent transcription factor targeted by PLZF. Pbx1 was highly expressed in the A375 and 397 cell lines, and its expression was markedly reduced by the expression of PLZF. Moreover, we showed that the growth suppression caused by ectopic expression of PLZF is reversed by enforced expression of Pbx1. Knockdown of Pbx1 using siRNAs in A375 and 397 cells reduced its protein levels by approximately 80%. Pbx1 siRNAs significantly inhibited cell growth in culture, thus suggesting that Pbx1 is a downstream target of PLZF in melanoma cell growth regulation.

In order to determine whether PLZF suppresses Pbx1 gene expression directly or indirectly, we examined the ability of PLZF to repress the Pbx1 promoter. We found that the 3.0 kb upstream region of the Pbx1 gene (nucleotides −3.0 kb to 0) contains seven possible PLZF DNA-binding consensus sequences. We then performed reporter assay and EMSA to examine the direct binding of PLZF in the Pbx1 promoter region. EMSA suggested the presence of an interactive site (Site 1) for PLZF in the 3.0-kb of upstream Pbx1 gene sequences. Deletion of Site 1, however, did not recover Pbx1 gene expression. These data suggest multiple direct and/or indirect regulation mechanisms for Pbx1 gene expression by PLZF. Further analysis is required for elucidating these mechanisms.

Pbx1 was originally identified at t(1;19) chromosomal translocations in acute pre-B-cell leukemias (Kamps *et al.*, 1990; Nourse *et al.*, 1990), and it has also been described as a transcriptional activator. Pbx1 is known to interact with a number of Hox proteins through the YPWM motif located at the N-termini of the homeodomains in Hox proteins and to regulate the function of Hox proteins (Chang *et al.*, 1995; Shanmugam *et al.*, 1997). It has been reported that Pbx1 cooperates in the cellular proliferation and transformation induced by Hox proteins (Krosl *et al.*, 1998). Krosl *et al.* (1998) showed that the ability of HoxB4 and HoxB3 to interact with Pbx1 is critical for transformation of Rat-1 cells, that Hox proteins have a notable effect on cell growth, and that Pbx1 further enhances this effect. Although HoxB7 is reportedly involved in melanoma growth (Care *et al.*, 1996, 2001; Felicetti *et al.*, 2004), there have been few reports on the relationship between Pbx1 and the progression of melanoma. We showed here that immunoprecipitation of HoxB7 from A375 and 397 melanoma cell lines co-precipitated a 52-kDa protein that was recognized by an anti-Pbx1 antibody, thus suggesting that Pbx1 physically interacts with HoxB7. Our data indicate that Pbx1 plays an important role in melanoma growth and that it forms heterocomplexes with HoxB7, which suggests that molecular events mediated by the Pbx1–HoxB7 heterocomplex are altered in melanoma cells when Pbx1 is suppressed by PLZF.

Previous studies have identified some HoxB7 target genes. bFGF was identified as the main target of HoxB7 in melanoma cell lines (Care *et al.*, 1996). In addition, VEGF, GROα, IL-8, Ang-2 and MMP9 were found to be upregulated in HoxB7-transduced cells (Care *et al.*, 2001). Based on these reports, we analysed the effect of Pbx1 knockdown on HoxB7 target genes. We found that knockdown of Pbx1 slightly downregulated HoxB7 itself and substantially downregulated bFGF, Ang-2 and MMP9, but not VEGF, GROα or IL-8. This suggests that HoxB7 target genes are differentially regulated by HoxB7–Pbx1 or by another HoxB7 complex. Interestingly, these factors are strongly associated with tumor angiogenesis and invasion (Becker *et al.*, 1989; Ahmad *et al.*, 2001; Etoh *et al.*, 2001; Johnson *et al.*, 2004). The Pbx1–HoxB7 complex may

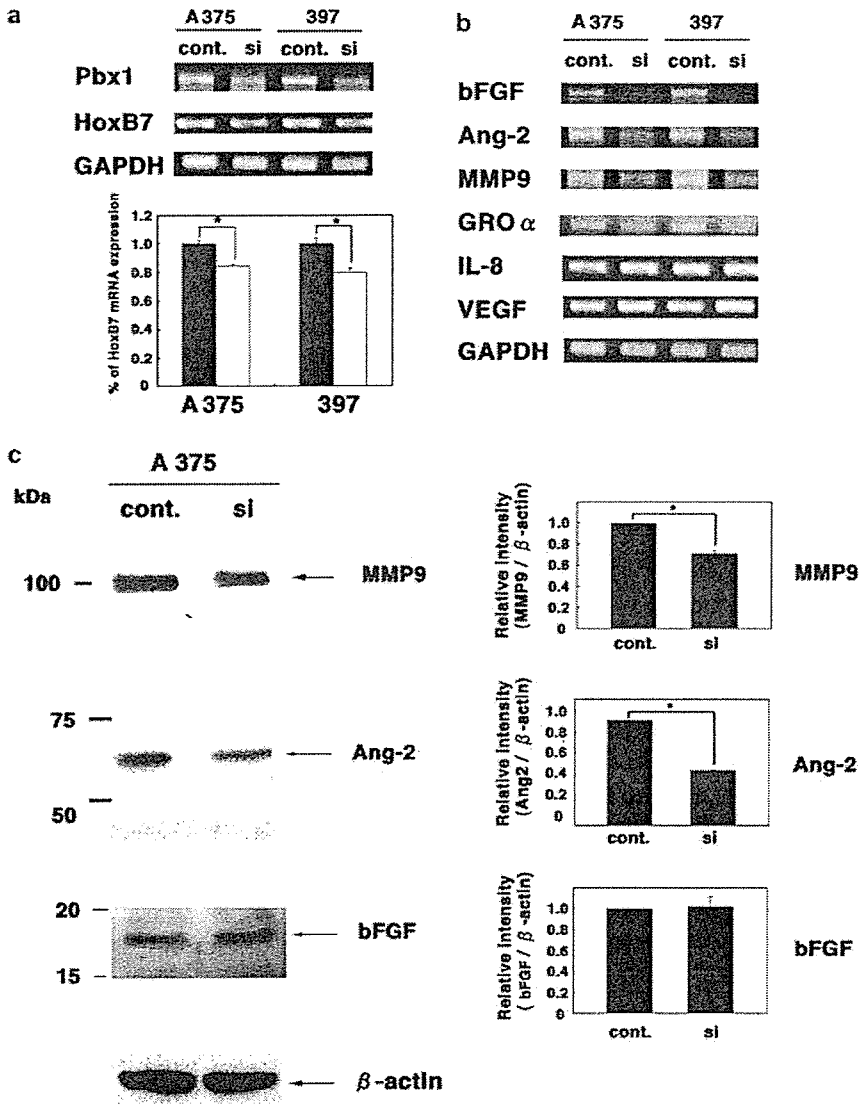

Figure 6 Expression of HoxB7 and its target genes is modulated by knockdown of Pbx1. (**a**) Upper panel: RT–PCR analysis of HoxB7 expression in Pbx1-knockdown melanoma cells and control cells. Lower panel: Relative intensity of Pbx1 and HoxB7 mRNA expression in Pbx1-knockdown melanoma cells and control cells, which was calculated as a ratio vs the expression of GAPDH. $^*P<0.05$. (**b**) RT–PCR analysis of HoxB7 target gene expression in each cell type. (**c**) Immunoblot analysis of Ang-2, MMP9 and bFGF in Pbx1-knockdown melanoma cells and control cells. Relative intensity of each protein was calculated as a ratio vs the expression of β-actin. $^*P<0.05$.

thus play a very important role in melanoma growth, and its suppression could be a major cause of the reduction in PLZF-mediated growth in melanoma. This is supported by previous reports that PLZF is expressed in melanocytes but not in melanoma cells, and that the pattern of PLZF expression inversely correlates with that of HoxB7 (Care *et al*., 1996, 1998).

In this study, we showed that the suppression of Pbx1 expression by PLZF downregulates some HoxB7 target genes, including bFGF, Ang-2 and MMP9. The data indicated that the changes in the molecular network caused by the loss of PLZF may play an important role in the progression of melanoma. Further analyses of the PLZF–Pbx1 network will assist in the discovery of target molecules for the development of novel anti-melanoma drugs.

Materials and methods

Materials

Human melanoma cell lines A375 and 397 were generously provided by Dr Kawakami (Keio University, Tokyo, Japan) (Sumimoto *et al*., 2004). Cells were grown in Roswell Park Memorial Institute medium 1640 supplemented with 10% fetal calf serum (FCS), penicillin (100 U/ml) and streptomycin

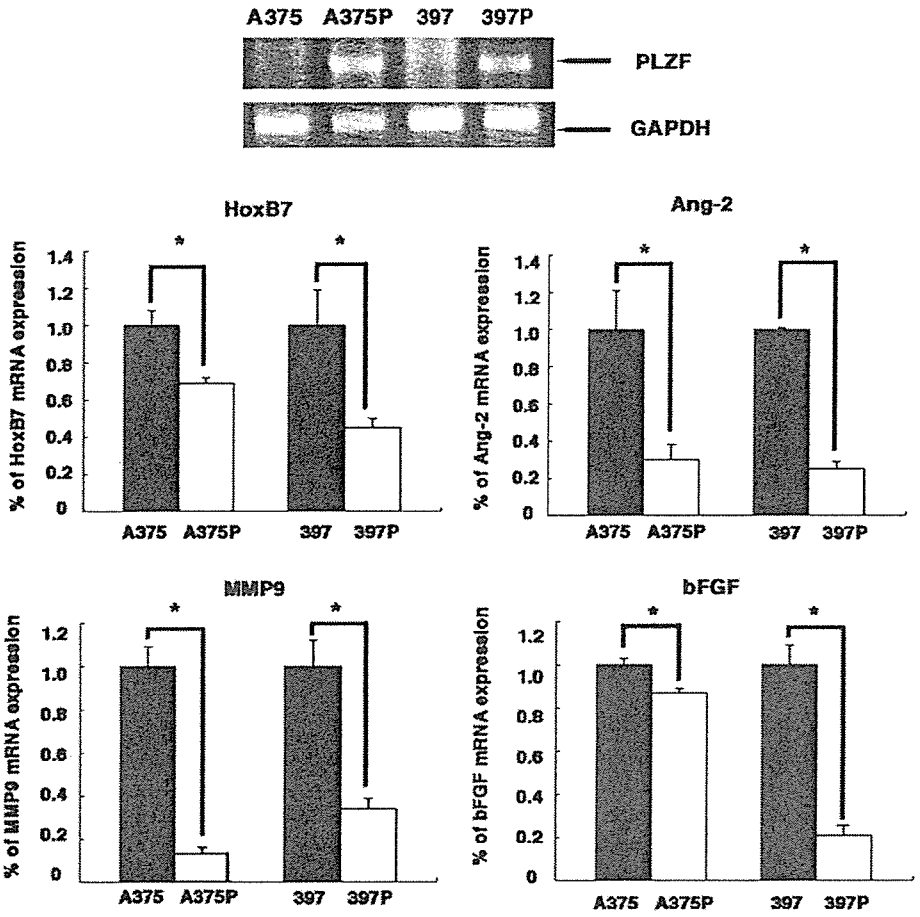

Figure 7 Expression of HoxB7, bFGF, Ang-2 and MMP9 is suppressed by the transduction of PLZF in melanoma cells. Upper panel: RT–PCR analysis for PLZF mRNA in A375, A375P, 397 and 397P cells. GAPDH, glyceraldehyde 3-phosphate dehydrogenase. PLZF was evaluated at 35 cycles, whereas control GAPDH evaluated at 24 cycles. Lower panel: qRT–PCR for HoxB7, bFGF, Ang-2 and MMP9 mRNA in PLZF-expressing melanoma cells and parental cells. $^*P<0.05$.

sulfate (100 μg/ml) at 37°C in an atmosphere containing 5% CO_2. Antibodies used were as follows: rabbit anti-Pbx1 polyclonal antibody (Santa Cruz Biotechnology, Santa Cruz, CA, USA), mouse anti-PLZF monoclonal antibody (Oncogene Research Products, San Diego, CA, USA), rabbit anti-HoxB7 polyclonal antibody (CeMines, Golden, CO, USA), rabbit anti-bFGF polyclonal antibody (Abcam, Cambridge, UK), mouse anti-Ang-2 monoclonal antibody, goat anti-MMP9 monoclonal antibody (R&D, Tokyo, Japan), goat horseradish peroxidase-conjugated anti-rabbit antibody, donkey horseradish peroxidase-conjugated anti-goat antibody and goat horseradish peroxidase-conjugated anti-mouse antibody (Promega, Madison, WI, USA).

Plasmid and adenovirus vector construction

A plasmid encoding PLZF was generated by subcloning the human PLZF cDNA into pcDNA3.1/Hygro. (Invitrogen, Carlsbad, CA, USA). A plasmid encoding Pbx1 was generated by subcloning Pbx1 cDNA into pME18S (Tanaka *et al*., 2004). The Pbx1 promoter 3.0 kb was subcloned into pGL3 (Promega). Transfection of plasmids was performed with LipofectAMINE (Invitrogen) according to the manufacturer's instructions. To assess transfection efficiency of pME18S-Pbx1 in 375P cells, both PME18S-Pbx1 and pME18S-ECFP plasmids were transfected into 375P cells and CFP-positive cells were counted. Adenovirus vector (Ax) carrying PLZF was prepared using an adenovirus expression vector kit (Takara Biomedicals, Kyoto, Japan). PLZF was subcloned into the cosmid cassette pAxCAw. Ax containing the CA promoter and PLZF (AxPLZF) was generated by the COS-TPC method according to the manufacturer's protocol. A375 and 397 cells were infected with Axs at an MOI of 50–200 for 1 h. Ax expressing LacZ (Ax-LacZ) and GFP (Ax-GFP) were used as controls to exclude the effects of Ax itself.

RT–PCR and quantitative real-time PCR

Primer sequences for RT–PCR are listed in Table 2. Total RNA was isolated from cultured melanoma cells using Trizol Reagent (Invitrogen), and was treated with DNase I (Clontech, Palo Alto, CA, USA) at 37°C for 30 min to remove contaminating genomic DNA. RT–PCR was performed using RT–PCR High Plus (Toyobo, Osaka, Japan) according to the manufacturer's instructions. cDNA was reverse transcribed from total RNA for 30 min at 60°C, and heated to 94°C for 2 min. Amplification was performed using a GeneAmp PCR System 9700 (Applied Biosystems, Foster City, CA, USA) for

Table 2 Primer sequences used in this study

Gene	*Upper primer (5′–3′)*	*Lower primer (5′–3′)*
Pbx1	GGAGATTGAGCGGATGGT	CATGGGCTGACACATTGGTAG
HoxB7	AAGGAGCAGAGGGACTCGGACT	AAATCTTGATCTGTCTTTCCGTGAG
bFGF	CCCAAGCGGCTGTAC	ATACTGCCCAGTTCGTTTCA
Ang-2	GCAGCCTATAACAACTTTCGGAAGA	TATTTCTATCATCACAGCCGTCT
MMP9	GAGATGCGTGGAGAGTCGAAA	CAAAGGCGTCGTCAATCA
GROα	ACTGCTGCTCCTGCTCCTGGTAGCC	TTTCCGCCCATTCTTGAGTGT
IL-8	GAATCTAAATTATCAGTCATA	CAGTGAACATTATAGATCTAT
VEGF	CTGCTGTCTTGGGTGCATTG	TCACCGCCTCGGCTTGTCACA
GAPDH	CGTATTGGGCGCCTGGTCACCAG	TCGCTCCTGGAAGATGGTGATGGG

Abbreviations: Ang-2, angiopoietin-2; bFGF, basic fibroblast growth factor; GAPDH, glyceraldehyde-3-phosphate dehydrogenase; GROα, growth-related oncogene-α; IL-8, interleukin-8; MMP9, matrix metalloprotease 9; Pbx1, pre-B-cell leukemia transcription factor 1; VEGF, vascular endothelial growth factor.

24 or 35 cycles. The cycle profile consisted of 1 min at 94°C for denaturation and 1.5 min at 60°C for annealing and primer extension. To evaluate amplification, 5 μl of the reaction mixture was electrophoresed on a 1.0% agarose gel containing ethidium bromide. We performed at least three independent studies and confirmed similar results. Quantitative real-time PCR (qRT–PCR) was performed using the ABI PRISM 7700 sequencer detection system (Perkin–Elmer Applied Biosystems, Foster City, CA, USA). Primers and probe were purchased from Applied Biosystems (Assays-on-Demand). RT–PCR mixtures were prepared according to the manufacturer's instructions for the TaqMan One-Step RT–PCR Master Mix Reagent kit (Perkin–Elmer Applied Biosystems). Probe was labeled with a reporter fluorescent dye (6-carboxyfluorescein) at the 5′ end. For glyceraldehyde 3-phosphate dehydrogenase (GAPDH) detection, Pre-Developed TaqMan Assay Reagent (Perkin–Elmer Applied Biosystems) was added. The thermal conditions were 48°C for 30 min for RT and 95°C for 10 min, followed by 45 amplification cycles of 95°C for 15 s for denaturing and 60°C for 1 min for annealing and extension. PCR products were sequenced to confirm proper amplification. To compare mRNA expression, results were determined as relative values against GAPDH as an internal reference. There were $n=3$ samples in each group.

siRNA experiments

siRNA sequences used in this study were as follows: Pbx1 siRNA sequences were 5′-CCGCAGGGCATCAGTGCTA-3′ (siRNA1) and 5′-CGACAGAAATCCTGAATGA-3′ (siRNA2), and the mutated Pbx1 siRNA sequences were 5′-CC ACAAGGCATTAGCGCTA-3′ (mut. siRNA1) and 5′-CG ACCGAGATCCTAAACGA-3′ (mut. siRNA2) (B-Bridge International, Sunnyvale, CA, USA). Scrambled siRNA directed against 5′-GCGCGCTTTGTAGGATTCG-3′ was also used as a negative control. This sequence was not present in any mammalian mRNAs in the National Center for Biotechnology Information database. siRNA transfection was performed with CodeBreaker siRNA Transfection Reagent (Promega). Briefly, cells (5×10^5) were incubated in 35-mm plates with siRNA (final concentration, 40 nM)–CodeBreaker Reagent (15 μl) mixture in serum-free medium for 24 h. Cells were then grown in media with 10% FCS.

Microarray analysis

Total RNA was isolated from LacZ or PLZF Ax-infected melanoma cells at 48 h post-infection. The Acegene Human oligo chip 30K (Hitachi Software Engineering, Yokohama, Japan) containing 30 000 genes was used to compare gene expression in melanoma cells infected with PLZF or LacZ adenovirus. Arrays were screened according to the manufacturer's protocol. Fluorescent images of hybridized microarrays were obtained with a CRBIO IIe microarray scanner (Hitachi Software Engineering), and images were analysed with DNAsis Array software (Hitachi Software Engineering).

EMSA

Nuclear protein extracts were prepared using celLytic NuCLEAR Extraction Kit (Sigma, St Louis, MO, USA). Biotin-labeled oligomers containing PLZF-binding sequences (Sites 1, 2, 3, 4, 5, 6 and 7) were bound to nuclear extracts. Binding reactions were performed using the LightShift EMSA Optimization and Control kit (Pierce, Rockford, IL, USA) according to the manufacturer's instructions. Reaction mixtures were incubated on ice for 60 min. Biotin-unlabeled oligomers were used as competitors, and when present, were added to the mixtures 30 min before the other reagents. Binding reactions were subjected to EMSA on 4% non-denaturing polyacrylamide gels in 0.5 × Tris-Borate-EDTA buffer, and detection was performed using a LightShift Chemiluminescent EMSA Kit (Pierce) according to the manufacturer's instructions. Sequences of the probes used in this study were as follows: Site 1, 5′-CCTCCAGATCCAGTT CATCC-3′; Site 2, 5′-CGGGGTAAGACAGTTGCAAT-3′; Site 3, 5′-TTTGAGTATATAGTTTTGTG-3′; Site 4, 5′-TTTAAAAAAACAGTTTAAAA-3′; Site 5, 5′-ACTGTG TACACAGTCAGATT-3′; Site 6 5′-AAAAATGACACA GTTTGGTA-3′; Site 7, 5′-GCTGGAACTACAGTAC CATT-3′ and mutated-Site 1, 5′-CCTCCAGAGAAAGTT CATCC-3′.

Luciferase reporter assays

Melanoma cells were cultured in 24-well plates and grown to 70% confluence. Cells were transfected with 0.8 μg/well of pGL3-Pbx1 plasmid DNA using LipofectAMINE (Invitrogen). Transfected cells were harvested at 24 h post-transfection, and lysates were assayed for luciferase activity with a Dual-Glo Luciferase Assay System (Promega) according to the manufacturer's protocol.

Immunoprecipitation and Western blotting

A375 and 397 cells were transiently transfected with pME18S-Pbx1 plasmid. Cells were lysed 48 h after transfection and equivalent amounts of lysate protein were subjected into immunoprecipitation. Immunoprecipitation and Western blotting were performed as described previously (Goishi *et al*.,

1995). After membranes were washed three times at intervals of 10 min with 0.05% Tween-20 in phosphate-buffered saline, horseradish peroxidase conjugate was detected by chemiluminescence with an ECL kit (Amersham, Buckinghamshire, UK) and autofluorography.

Acknowledgements

We thank Drs T Tsuda, T Jyokou, E Tan, M Tohyama, H Iwabuki, T Kikugawa, Y Kinugasa and E Koya for technical assistance, helpful comments and discussion.

References

Ahmad SA, Liu W, Jung YD, Fan F, Wilson M, Reinmuth N *et al.* (2001). The effects of angiopoietin-1 and -2 on tumor growth and angiogenesis in human colon cancer. *Cancer Res* **61**: 1255–1259.

Barna M, Hawe N, Niswander L, Pandolfi PP. (2000). Plzf regulates limb and axial skeletal patterning. *Nat Genet* **25**: 166–172.

Barna M, Merghoub T, Costoya JA, Ruggero D, Branford M, Bergia A *et al.* (2002). Plzf mediates transcriptional repression of HoxD gene expression through chromatin remodeling. *Dev cell* **3**: 499–510.

Becker D, Meier CB, Herlyn M. (1989). Proliferation of human malignant melanomas is inhibited by antisense oligodeoxynucleotides targeted against basic fibroblast growth factor. *EMBO J* **8**: 3685–3691.

Care A, Silvani A, Meccia E, Mattia G, Stoppacciaro A, Parmiani G *et al.* (1996). HOXB7 constitutively activates basic fibroblast growth factor in melanomas. *Mol Cell Biol* **16**: 4842–4851.

Care A, Silvani A, Meccia E, Mattia G, Peschle C, Colombo MP. (1998). Transduction of the SkBr3 breast carcinoma cell line with the HOXB7 gene induces bFGF expression, increases cell proliferation and reduces growth factor dependence. *Oncogene* **16**: 3285–3289.

Care A, Felicetti F, Meccia E, Bottero L, Parenza M, Stoppacciaro A *et al.* (2001). HOXB7: a key factor for tumor-associated angiogenic switch. *Cancer Res* **61**: 6532–6539.

Chang CP, Shen WF, Rozenfeld S, Lawrence HJ, Largman C, Cleary ML. (1995). Pbx proteins display hexapeptide-dependent cooperative DNA binding with a subset of Hox proteins. *Genes Dev* **9**: 663–674.

Chen Z, Brand NJ, Chen A, Chen SJ, Tong JH, Wang ZY *et al.* (1993). Fusion between a novel Kruppel-like zinc finger gene and the retinoic acid receptor-alpha locus due to a variant t(11;17) translocation associated with acute promyelocytic leukaemia. *EMBO J* **12**: 1161–1167.

Costoya JA, Hobbs RM, Barna M, Cattoretti G, Manova K, Sukhwani M *et al.* (2004). Essential role of Plzf in maintenance of spermatogonial stem cells. *Nat Genet* **36**: 653–659.

Etoh T, Inoue H, Tanaka S, Barnard GF, Kitano S, Mori M. (2001). Angiopoietin-2 is related to tumor angiogenesis in gastric carcinoma: possible *in vivo* regulation via induction of proteases. *Cancer Res* **61**: 2145–2153.

Felicetti F, Bottero L, Felli N, Mattia G, Labbaye C, Alvino E *et al.* (2004). Role of PLZF in melanoma progression. *Oncogene* **23**: 4567–4576.

Goishi K, Higashiyama S, Klagsbrun M, Nakano N, Umata T, Ishikawa M *et al.* (1995). Phorbol ester induces the rapid processing of cell surface heparin-binding EGF-like growth factor: conversion from juxtacrine to paracrine growth factor activity. *Mol Biol Cell* **6**: 967–980.

Heinemeyer T, Wingender E, Reuter I, Hermjakob H, Kel AE, Kel OV *et al.* (1998). Databases on transcriptional regulation: TRANSFAC, TRRD and COMPEL. *Nucleic Acids Res* **26**: 364–370.

Hong SH, David G, Wong CW, Dejean A, Privalsky ML. (1997). SMRT corepressor interacts with PLZF and with the PML-retinoic acid receptor alpha (RARalpha) and PLZF-RARalpha oncoproteins associated with acute promyelocytic leukemia. *Proc Natl Acad Sci USA* **94**: 9028–9033.

Johnson C, Sung HJ, Lessner SM, Fini ME, Galis ZS. (2004). Matrix metalloproteinase-9 is required for adequate angiogenic revascularization of ischemic tissues: potential role in capillary branching. *Circ Res* **94**: 262–268.

Kamps MP, Murre C, Sun XH, Baltimore D. (1990). A new homeobox gene contributes the DNA binding domain of the t(1;19) translocation protein in pre-B ALL. *Cell* **60**: 547–555.

Krosl J, Baban S, Krosl G, Rozenfeld S, Largman C, Sauvageau G. (1998). Cellular proliferation and transformation induced by HOXB4 and HOXB3 proteins involves cooperation with PBX1. *Oncogene* **16**: 3403–3412.

Li JY, English MA, Ball HJ, Yeyati PL, Waxman S, Licht JD. (1997). Sequence-specific DNA binding and transcriptional regulation by the promyelocytic leukemia zinc finger protein. *J Biol Chem* **272**: 22447–22455.

Mann RS, Chan SK. (1996). Extra specificity from extradenticle: the partnership between HOX and PBX/EXD homeodomain proteins. *Trends Genet* **12**: 258–262.

McConnell MJ, Chevallier N, Berkofsky-Fessler W, Giltnane JM, Malani RB, Staudt LM *et al.* (2003). Growth suppression by acute promyelocytic leukemia-associated protein PLZF is mediated by repression of c-*myc* expression. *Mol Cell Biol* **23**: 9375–9388.

Nourse J, Mellentin JD, Galili N, Wilkinson J, Stanbridge E, Smith SD *et al.* (1990). Chromosomal translocation t(1;19) results in synthesis of a homeobox fusion mRNA that codes for a potential chimeric transcription factor. *Cell* **60**: 535–546.

Shanmugam K, Featherstone MS, Saragovi HU. (1997). Residues flanking the HOX YPWM motif contribute to cooperative interactions with PBX. *J Biol Chem* **272**: 19081–19087.

Sumimoto H, Miyagishi M, Miyoshi H, Yamagata S, Shimizu A, Taira K *et al.* (2004). Inhibition of growth and invasive ability of melanoma by inactivation of mutated BRAF with lentivirus-mediated RNA interference. *Oncogene* **23**: 6031–6039.

Tanaka M, Nanba D, Mori S, Shiba F, Ishiguro H, Yoshino K *et al.* (2004). ADAM binding protein Eve-1 is required for ectodomain shedding of epidermal growth factor receptor ligands. *J Biol Chem* **279**: 41950–41959.

Wong CW, Privalsky ML. (1998). Components of the SMRT corepressor complex exhibit distinctive interactions with the POZ domain oncoproteins PLZF, PLZF-RARalpha, and BCL-6. *J Biol Chem* **273**: 27695–27702.

Yeyati PL, Shaknovich R, Boterashvili S, Li J, Ball HJ, Waxman S *et al.* (1999). Leukemia translocation protein PLZF inhibits cell growth and expression of cyclin A. *Oncogene* **18**: 925–934.

Journal of Dermatological Science (2007) 45, 69–72

ELSEVIER

Journal of Dermatological SCIENCE

www.intl.elsevierhealth.com/journals/jods

LETTER TO THE EDITOR

Epiregulin, a member of the EGF family, is over-expressed in psoriatic epidermis

KEYWORDS
Epiregulin; EGF family; Psoriasis; TGF-α; Amphiregulin; Northern blot; *In situ* hybridization

Psoriasis is characterized by the hyperproliferation of keratinocytes, altered epidermal differentiation, dermal angiogenesis, and a dense lesional infiltrate in the dermal and epidermal component, consisting mainly of macrophages, lymphocytes, and neutrophils. To date, the expression of many regulatory molecules has been well clarified in psoriatic epidermis. Previous reports have shown that various cytokines and growth factors are over-expressed in psoriatic epidermis [1]. Keratinocytes are the main component cells of the epidermis, and their growth is regulated by both positive and negative mediators [2]. Of these mediators, the most important mechanism for the proliferation of keratinocytes is the signal from the epidermal growth factor (EGF) receptor. The EGF family consists of EGF, transforming growth factor-α (TGF-α), heparin binding EGF-like growth factor (HB-EGF), amphiregulin, epiregulin, betacellulin, epigen, neuregulin (NRG)-1, NRG-2, NRG-3, and NRG-4, and the EGF receptor (EGFR) family consists of EGFR (also called ErbB1), ErbB2, ErbB3, and ErbB4 [2]. Previous reports have shown that TGF-α, amphiregulin and HB-EGF are over-expressed in psoriatic epidermis [3–5]. Given that epiregulin is a member of the EGF family and an autocrine growth factor for normal human keratinocytes [6], we speculated that epiregulin is over-expressed in psoriasis. To prove our hypothesis, we investigated the expression of epiregulin as well as TGF-α and amphiregulin in psoriatic epidermis.

All procedures that involved human subjects received prior approval from the Ethics Committee of Ehime University School of Medicine, Toon, Ehime, Japan, and all subjects provided written informed consent. Twelve psoriatic lesional skin samples and 10 normal healthy skin samples were obtained. To exclude the RNA from the dermis, we separated the epidermis from the dermis by a heat-separation technique. The specimens were heated at 60 °C in sterile saline for 1 min. The epidermis was then separated from the dermis, immediately frozen in liquid nitrogen. We confirmed that heat-separation did not influence on the results. Total RNA was extracted from snap-frozen epidermis by using Isogen (Nippon Gene, Tokyo, Japan). Northern blot analysis was performed as previously described [6]. TGF-α mRNA was detected in all the psoriatic

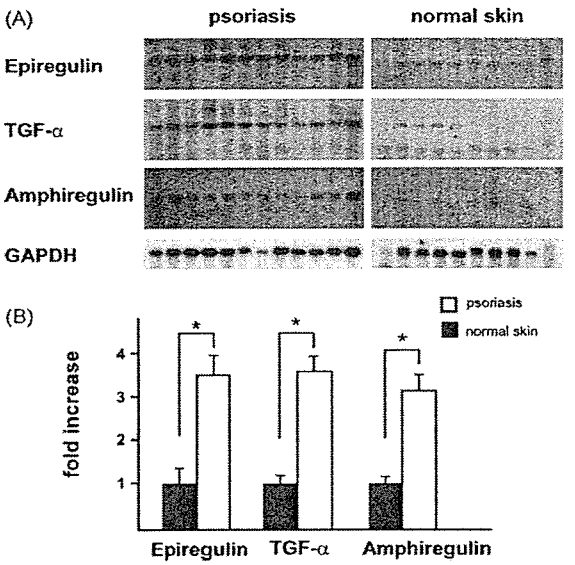

Fig. 1 mRNA expression of epiregulin, TGF-α, and amphiregulin in psoriatic epidermis. (A) The mRNA expression levels of epiregulin, TGF-α, and amphiregulin were analyzed by Northern blotting in psoriatic and normal epidermis. (B) Densitometric analysis of Northern blotting. Quantification of the signals was performed by using a densitometer and analyzed by ImageQuant software. Normal epidermis signal values were taken as 100% control. The signals were adjusted by GAPDH as an internal standard. $^{*}p < 0.05$.

doi:10.1016/j.jdermsci.2006.08.010

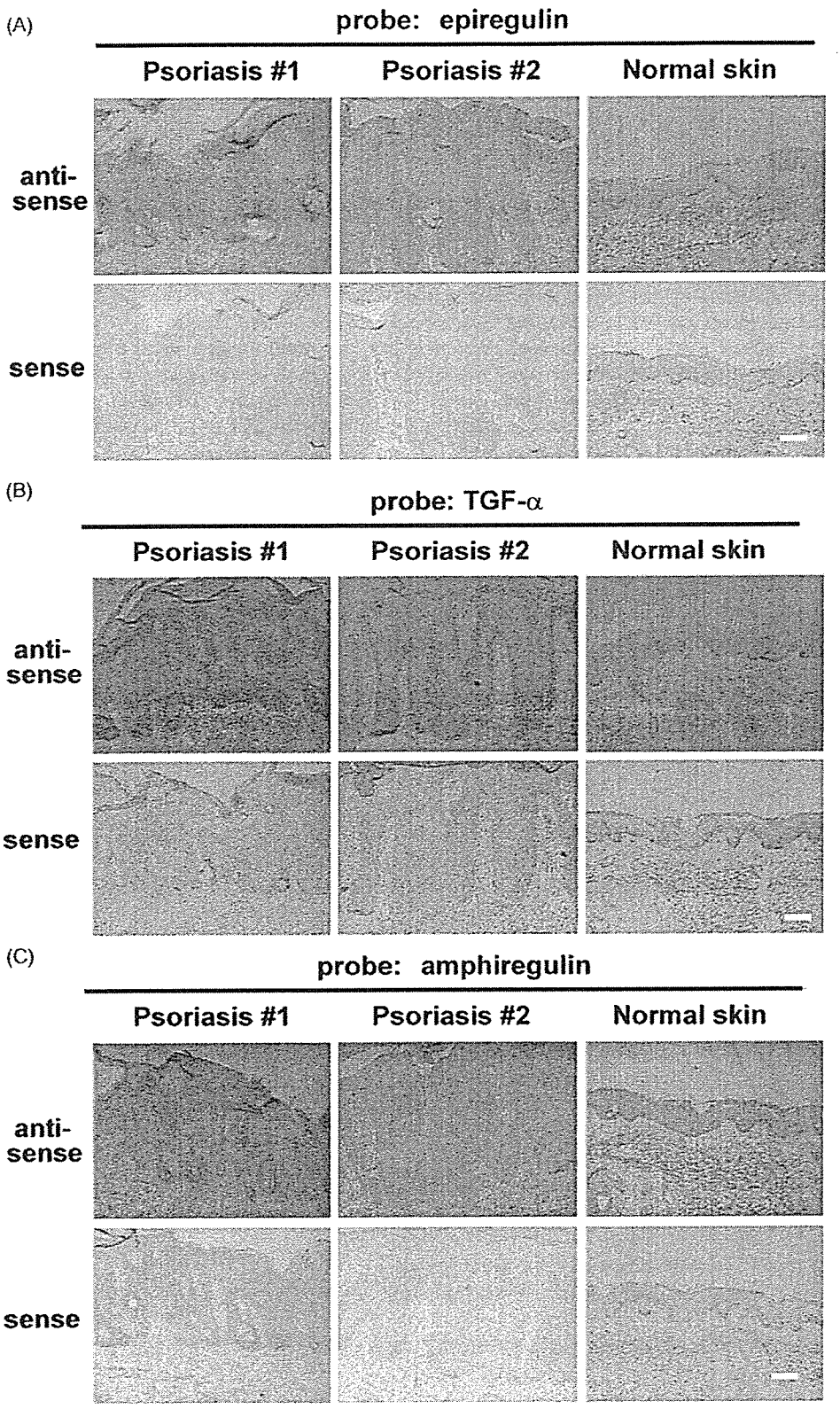

Fig. 2 *In situ* hybridization of epiregulin, TGF-α, and amphiregulin in psoriatic epidermis. *In situ* hybridization was performed using an automated *in situ* hybridization protocol. (A) Epiregulin; (B) TGF-α; (C) amphiregulin. Bar: 100 μm.

epidermis samples and was expressed at higher levels than in the normal epidermis. Amphiregulin mRNA was also detected in all the psoriatic epidermis samples and was expressed at higher levels than in the normal epidermis. The 4.8-kb transcript of epiregulin was detected in both normal and psoriatic epidermis, although the expression level was higher in the psoriatic epidermis than in the normal epidermis (Fig. 1A). Densitometric analysis revealed that TGF-α and amphiregulin mRNA were elevated by 3.6- and 3.2-fold, respectively. Epiregulin mRNA was also increased in psoriatic epidermis by 3.5-fold (Fig. 1B). To identify the localization of epiregulin, TGF-α, and amphiregulin mRNA, we performed *in situ* hybridization as previously described [7]. In normal skin, we found that epiregulin mRNA was expressed in the basal layer and that its expression was very faint. However, epiregulin mRNA was over-expressed in the spinous layer, mainly in the uppermost region of the spinous layer, but not in the basal layer of the psoriatic lesional epidermis (Fig. 2A). TGF-α and amphiregulin mRNA were also over-expressed in the spinous layer, but not in the basal layer, of the psoriatic lesional epidermis (Fig. 2B and C).

Considerable evidence currently exists to support the concept that psoriasis is mediated by many inflammatory cytokines. There is a predominance of Th1 cytokines, mainly interferon gamma (IFN-γ), in contrast to the predominance of Th2 cytokines found in atopic dermatitis. This immune-mediated aspect of psoriasis pathogenesis has been confirmed by the use of cyclosporine or targeted therapies against T cells, CD11a, or TNF-α [1]. With regard to keratinocytes, psoriatic plaques represent a hyperproliferative condition and deregulated differentiation [1]. Keratinocytes are the main component cells of the epidermis, and the important mechanism for keratinocyte growth is the EGF receptor-ligand system. In this EGF receptor-ligand system, the signal from ErbB1 (EGFR) is important for keratinocyte growth. TGF-α, HB-EGF, amphiregulin and epiregulin are autocrine growth factors and all bind to ErbB1 [2]. Previous reports have shown that TGF-α and amphiregulin mRNA are over-expressed in psoriatic lesional skin and play important roles for the keratinocyte proliferation of psoriatic epidermis, suggesting that all members of the EGF family are up-regulated in psoriatic epidermis [3–5]. In this study, we investigated the mRNA expression of epiregulin as well as TGF-α and amphiregulin in psoriatic and normal epidermis. The mRNA expression of TGF-α and amphiregulin was elevated in psoriatic epidermis, as compared to normal skin, as previously reported. The mRNA expression of epiregulin was also increased in psoriatic epidermis. Over-expressed epiregulin mRNA was localized in the spinous layer, but not in the basal layer, of the psoriatic epidermis. TGF-α and amphiregulin mRNA localization in psoriatic epidermis is within the spinous layer. This deregulated growth factor signaling may contribute to the hyperproliferative condition of psoriasis. In fact, a transgenic mouse with the amphiregulin gene revealed a psoriasis-like phenotype [8]. Based on our results and previous reports, a cross-induction mechanism of the keratinocyte-derived EGF family is involved in the development of psoriatic hyperproliferative epidermis.

Intracellular signaling systems such as Erk/JNK or MAP kinase, which are activated by the EGF family, are up-regulated in psoriatic epidermis [9]. Recent studies have shown that transgenic mice over-expressing a constitutive active form of STAT3 develop a psoriasis-like phenotype [10]. Because these molecules are downstream of EGFR signaling, an over-expressed EGF family may contribute to the pathogenesis of psoriasis by activating signal transduction molecules. Because topical treatment will probably remain the mainstay of psoriasis therapy for most patients, and aberrant expression of epiregulin as well as TGF-α and amphiregulin could facilitate the development of proliferative pathological conditions of psoriasis, additional targeting of such signal transduction molecule and/or growth factors may enhance anti-psoriatic therapy.

In conclusion, we have demonstrated the over-expression of epiregulin in psoriatic epidermis. Autocrine EGF-related growth factors may play an important role in the pathogenesis of psoriasis.

Acknowledgments

This work was partly supported by Health Sciences Research Grants for Research on Specific Diseases from the Ministry of Health, Labor, and Welfare of Japan and a Grant-in-Aid for Scientific Research from the Ministry of Education, Culture, Sports, Science, and Technology of Japan. We would also like to thank Teruko Tsuda and Eriko Tan for their technical assistance.

References

[1] Schon MP, Boehncke WH. Psoriasis. N Engl J Med 2005;352:1899–912.
[2] Hashimoto K. Regulation of keratinocyte function by growth factors. J Dermatol Sci 2000;24:S46–50.
[3] Cook PW, Pittelkow MR, Keeble WW, Graves-Deal R, Coffey Jr RJ, Shipley GD. Amphiregulin messenger RNA is elevated

in psoriatic epidermis and gastrointestinal carcinomas. Cancer Res 1992;52:3224–7.
[4] Elder JT, Fisher GJ, Lindquist PB, Bennett GL, Pittelkow MR, Coffey Jr RJ, et al. Overexpression of transforming growth factor alpha in psoriatic epidermis. Science 1989;243:811–4.
[5] Stoll SW, Elder JT. Retinoid regulation of heparin-binding EGF-like growth factor gene expression in human keratinocytes and skin. Exp Dermatol 1998;7:391–7.
[6] Shirakata Y, Komurasaki T, Toyoda H, Hanakawa Y, Yamasaki K, Tokumaru S, et al. Epiregulin, a novel member of the epidermal growth factor family, is an autocrine growth factor in normal human keratinocytes. J Biol Chem 2000;275:5748–53.
[7] Nitta H, Kishimoto J, Grogan TM. Application of automated mRNA in situ hybridization for formalin-fixed, paraffin-embedded mouse skin sections: effects of heat and enzyme pretreatment on mRNA signal detection. Appl Immunohistochem Mol Morphol 2003;11: 183–7.
[8] Cook PW, Piepkorn M, Clegg CH, Plowman GD, DeMay JM, Brown JR, et al. Transgenic expression of the human amphiregulin gene induces a psoriasis-like phenotype. J Clin Invest 1997;100:2286–94.
[9] Zhang X, Yang D, Ma S, Liu H. Up-regulation of activities of mitogen-activated protein kinase in psoriatic lesions. J Dermatol Sci 2005;37:118–9.
[10] Sano S, Chan KS, Carbajal S, Clifford J, Peavey M, Kiguchi K, et al. Stat3 links activated keratinocytes and immunocytes required for development of psoriasis in a novel transgenic mouse model. Nat Med 2005;11: 43–9.

Yuji Shirakata*
Department of Dermatology, Ehime University School of Medicine, Shitsukawa, Toon, Ehime 791-0295, Japan

Jiro Kishimoto
Shiseido Research Center, Tsuzuki-ku, Yokohama, Kanagawa, Japan

Sho Tokumaru
Kenshi Yamasaki
Yasushi Hanakawa
Mikiko Tohyama
Koji Sayama
Koji Hashimoto
Department of Dermatology, Ehime University School of Medicine, Shitsukawa, Toon, Ehime 791-0295, Japan

*Corresponding author.
Tel.: +81 89 960 5350;
fax: +81 89 960 5352
E-mail address: shirakat@m.ehime-u.ac.jp
(Y. Shirakata)

19 April 2006

Cell Tissue Res (2006) 326: 69–77
DOI 10.1007/s00441-006-0208-2

REGULAR ARTICLE

Lujun Yang · Yuji Shirakata · Masachika Shudou · Xiuju Dai · Sho Tokumaru · Satoshi Hirakawa · Koji Sayama · Junji Hamuro · Koji Hashimoto

New skin-equivalent model from de-epithelialized amnion membrane

Received: 14 December 2005 / Accepted: 23 March 2006 / Published online: 7 June 2006

Abstract The presence of pre-existing basement membrane (BM) components improves the morphogenesis of epidermis and BM in constructing a human living skin-equivalent (LSE). De-epithelialized amniotic membrane (AM) retains key BM components. We have therefore investigated the usefulness of AM for constructing LSE. De-epithelialized AM was overlaid on type I collagen gel embedded with fibroblasts. Normal human keratinocytes (NHKs) were then seeded onto the epithelial side of the AM to construct an AM-LSE. A conventional LSE was constructed by seeding NHKs on a fibroblast-populated type I collagen gel. When the keratinocytes reached confluence, the LSE was lifted to the air-liquid interface and cultured for up to 3 weeks. Samples were harvested at various times and investigated morphologically, immunohistochemically, and ultrastructurally. In AM-LSE, the epidermis was better stratified, with more compact, polarized, columnar basal cells, and the expression of differentiation and proliferation markers was more similar to that of normal human skin than was that of LSE without AM. A more continuous BM and better-developed hemidesmosomes were found in AM-LSE. The epidermis of AM-LSE outgrew much faster than that of LSE without AM. When transplanted onto nude mice, both LSEs took well; however, the AM-LSE graft showed better morphogenesis of the epidermis, BM, and hemidesmosomes. The better epidermal morphology and better-developed BM in AM-LSE in vitro and in vivo indicates its superiority over LSE without AM for clinical applications.

Keywords Amniotic membrane · Basement membrane · Keratinocyte · Migration · Skin-equivalent · Human · Mouse (BALB/cAJc1-nu)

This work was partly supported by Health Sciences Research Grants for Research on Specific Diseases from the Ministry of Health, Labor, and Welfare of Japan (to K.H.) and a Grant-in-Aid for Scientific Research from the Ministry of Education, Culture, Sports, Science, and Technology of Japan (to K.H. and Y.S.).
L. Yang and Y. Shirakata contributed equally to this work.

L. Yang · Y. Shirakata (✉) · X. Dai · S. Tokumaru · S. Hirakawa · K. Sayama · K. Hashimoto
Department of Dermatology,
Ehime University School of Medicine,
Shitsukawa,
Toon, Ehime 791-0295, Japan
e-mail: shirakat@m.ehime-u.ac.jp
Tel.: +81-89-9605350
Fax: +81-89-9605352

M. Shudou
Department of Bioscience, Ehime University,
Shitsukawa,
Toon, Ehime 791-0295, Japan

J. Hamuro
ArBlast,
Chuo-ku, Kobe 650-0047, Japan

Introduction

Living skin-equivalent (LSE), which consists of epidermis and dermis matrix, has long been used as a skin substitute for wound closure (Eaglstein and Falanga 1998). A well-developed differentiated epidermis provides a barrier against bacteria and other environmental factors, and the presence of a basement membrane (BM) and fibroblasts are necessary for maintaining epidermal architecture and sustaining growth (Andriani et al. 2003). A variety of biomaterials has been used to construct the dermal matrix of LSE (Guerret et al. 2003; Llames et al. 2004; Meana et al. 1998; Medalie et al. 1997; Ojeh et al. 2001), including type I collagen gel, fibrin gel, human plasma, and acellular human dermis. This shows that BM is not just an inert matrix that supports the epidermis, but that it also regulates epidermal morphogenesis and homeostasis via dynamic cross-talk with the overlying epidermis. Among dermal materials, acellular human dermis possesses an intact BM and supports the epidermis with good morphogenesis and a rete ridge-like pattern. The presence of pre-existing BM component proteins of the dermal matrix is essential for the development of the BM in an LSE (Ralston et al. 1999).

However, large amounts of human dermis are difficult to obtain for clinical application.

Amniotic membrane (AM) is composed of a single layer of columnar epithelial cells, a BM, an acellular compact layer, and the underlying fibroblast and spongy layers (von Versen-Hoynck et al. 2004). The BM zone underlying the amniotic epithelium resembles that of skin morphologically and ultrastructurally and consists of laminin 5 and types IV, VII, and XVII collagen (Oyama et al. 2003). As a biomaterial, AM is readily available and inexpensive and has been used to cover wounds temporarily, thereby reducing inflammation, facilitating epithelialization, and preventing scarring (Sheridan and Moreno 2001; Tseng 2001). De-epithelialized amnion has been employed as a carrier tissue for corneal or oral epithelial cell cultures to make a cornea-equivalent for ocular surface reconstruction (Nakamura et al. 2003a,b, 2004).

Since AM retains the major BM components, AM might be useful for constructing a better LSE. In this study, we have prepared de-epithelialized AM that retains the major BM components and have investigated whether AM improves the epidermis in an LSE. We have seeded keratinocytes onto AMs previously placed (epithelial side up) onto fibroblast-populated type I collagen gels, in order to construct an AM-LSE. Conventional LSEs have also been constructed from the same keratinocytes and fibroblasts by using the same protocol, except for the use of AM. We have further investigated the usefulness of AM for LSE in vitro and in vivo.

Materials and methods

Cell culture

Normal human epidermal keratinocytes (NHKs) were isolated from healthy human skin and cultured under serum-free conditions, as described previously (Shirakata et al. 2003, 2004). The cells were used for LSE cultures in their fourth passage. Fibroblasts were isolated from normal human skin and cultured in DMEM supplemented with 10% fetal calf serum (FCS), and 5th passage cells were used to construct the LSE. All procedures that involved human subjects received prior approval from the Ethics Committee of Ehime University School of Medicine, Toon, Ehime, Japan, and all subjects provided written informed consent.

Preparation of cultured skin-equivalents

The preparation of LSE has been described previously (Yang et al. 2005). Briefly, a collagen gel was prepared by mixing six volumes of ice-cold porcine collagen type I solution (Nitta Gelatin, Osaka, Japan) with one volume of 8×DMEM (Gibco), ten volumes of 1×DMEM supplemented with 20% FCS, and one volume of 0.1 N NaOH. Of this solution, 1 ml was added to each culture insert (Transwel-COL, membrane pore-size: 3 μm, Costar) in a 6-well culture plate (Costar). Following polymerization of the gel in the inserts at 37°C, two volumes of fibroblast suspension solution (5×10^5 cells/ml in 1×DMEM supplemented with 10% FCS) were added to eight volumes of the collagen solution (the final collagen concentration was 0.8 mg/ml), and then 3.5 ml of the fibroblast-containing collagen solution was applied to each insert. When the fibroblast-containing gel polymerized, DMEM supplemented with 10% FCS and ascorbic acid (final concentration: 50 ng/ml) was added. The gel was kept in submerged culture for 5 days, until the fibroblasts contracted the gel.

Human AM was obtained at cesarean section. Under sterile conditions, the AM was washed with sterile phosphate-buffered saline (PBS) and stored at −80°C in 12% dimethylsufoxide in PBS. Before use, the AM was thawed, washed three times with PBS, and cut into pieces (2.5×2.5 cm). The epithelial cells were removed from the AM by incubation in 0.02% EDTA at 37°C for 2 h and then gentle scraping with a cell scraper under a microscope. The spongy layer was also removed. The complete removal of the epithelial cells was confirmed by using hematoxylin and eosin (HE) staining.

The de-epithelialized AM was put, epithelial side up, onto the contracted gel surface, and a stainless steel ring (interior diameter: 11 mm) was overlaid on it to stabilize it. In the hole of the ring, 4×10^5 keratinocytes in 100 μl MCDB 153 type II were seeded onto the AM. The keratinocytes were maintained, submerged in culture, for 2 days. When the keratinocytes reached confluence, the LSE was lifted to the air-liquid interface and cornification medium (a 1:1 mixture of Ham's F-12 and DMEM supplemented with 2% FCS and other supplements; see Yang et al. 2005) was added. The medium was changed every other day. To construct a conventional LSE, keratinocytes were seeded onto the contracted gel and then submerged and airlifted as described above, except for the use of de-epithelialized AM. The stainless steel rings were used to adjust the seeding cell density. Both types of LSE were harvested 7 and 21 days after airlifting. For HE staining, the LSE was fixed in 20% formalin and embedded in paraffin. For immunohistochemical staining, the LSE was snap-frozen in OCT compound. We performed more than 20 experiments, with similar results being obtained in each (a representative experiment is shown in the figures). In comparative studies, keratinocytes and fibroblasts from the same donor were used.

Histology and immunohistochemical staining

Paraffin-embedded LSE samples were sectioned at 6 μm and stained with HE. For immunohistochemical staining, a Histofine Simple Stain MAX-PO (M) kit (Nichirei, Tokyo, Japan) was used according to the manufacturer's instructions. Frozen sections (7 μm) were first incubated with 0.3% hydrogen peroxide for 30 min to remove endogenous peroxidase activity and then incubated with primary antibodies at appropriate dilutions (Table 1) overnight at 4°C. The sections were incubated with enzyme-conjugated

secondary antibodies for 30 min at room temperature and then with the staining substrate. Images were obtained by using an Olympus AX80 microscope coupled with an Olympus DP50 digital camera (Olympus, Tokyo, Japan). We performed at least three independent studies and obtained similar results (a representative experiment is shown in the figures).

Evaluating the epidermal spreading potential of AM-LSEs

Stainless steel rings with an inner diameter of 6 mm were put on gels with or without AM, and 2×10^5 keratinocytes in 30 µl of MCDB 153 II medium were seeded in the hole of each ring. When the keratinocytes reached confluence, the LSEs were lifted to the air-liquid surface, and the stainless steel rings were removed. At days 0, 3, 5, 7, and 10 after being airlifted, epidermal size was measured by using a computer-assisted morphometric analysis. The epidermal size of the conventional and AM-LSEs was compared statistically by using Student's *t*-test.

Transplanting cultured LSEs

The animal grafting protocol was approved by the Ethics Committee of Ehime University School of Medicine. Eight-week-old female BALB/cAJcl-nu nude mice were anesthetized by intraperitoneal injection of 0.3 ml of Avertin (1.25% tribromoethanol, 2.5% 2-methyl-2-butanol solution). Full-thickness wounds were created on the skin of the backs of each mouse by using an 8-mm skin biopsy punch. A piece of AM-LSE or conventional LSE of matching size (7 days after airlift) obtained using the same punch was grafted onto the wound and covered with a transparent film. At 14 days after transplantation, the grafts were harvested. One part of each graft was paraffin-embedded and sectioned at 6 µm. Some sections were stained with HE, and some were de-paraffinized and blocked for endogenous peroxidase activity and then blood vessels were stained with rabbit antibody against type IV collagen (at dilution 1:50; American Research Products, Belmont, Mass.) according to the protocol of the Histofine SAB-AP (R) kit (Nichirei, Tokyo, Japan). Finally, the sections were counterstained with hematoxylin for cell nuclei. One part of each graft was also processed for electron-microscopic analysis. We performed at least three independent studies and obtained similar results (a representative experiment is shown in the figures).

Transmission electron microscopy

Specimens were fixed with 0.1% tannic acid, 2.5% glutaraldehyde in 0.1 M phosphate buffer (pH 7.4) for 2 h, washed with phosphate buffer, postfixed with 1% osmium tetroxide in phosphate buffer for 2 h, washed with 0.25 M sucrose solution, dehydrated in a graded series of ethanol, and embedded in an Epon-resin mixture. Ultrathin sections (<60–80 nm) were prepared by using a Leica Ultracut S, double-stained with uranyl acetate and lead citrate, and examined with a transmission electron microscope (JEM-1230, JEOL, Tokyo, Japan) at 80 kV.

Results

AM-LSE has a better-organized and more mature epidermis

Both AM-LSE and the conventional LSE showed differentiated epidermis with a basal layer, suprabasal layer, and stratum corneum at days 7 and 21 after airlifting (Fig. 1). The epidermal stratification was however better organized in the AM-LSE; the basal cells were cuboid, smaller, and more compact, and aligned along the AM with clear demarcation (Fig. 1a,b). In the conventional LSE, the epidermal stratification was not as well organized. The larger round basal cells were sparsely aligned along the dermal-epidermal junction, and the number of basal cells had decreased considerably by day 21 (Fig. 1e,f).

We found keratin 6, a marker of keratinocyte activation, only in hair follicles in normal human skin sections (Fig. 2). In AM-LSE, keratin 6 staining was faint at day 7 and disappeared almost completely in the basal and lower suprabasal layers by day 21 (Fig. 2a,k). In conventional LSE, the epidermis strongly expressed keratin 6 up to

Table 1 Details of primary antibodies used

Antigen	Clone	Dilution of antibody	Antibody source
E-cadherin	HECD-1	1:100	TaKaRa
Desmoglein 1	27B2	1:100	Zymed
Desmoglein 3	5G11	1:100	Zymed
Keratin 10	LHP1	1:100	NeoMarkers
Keratin 6	LHK6B	1:100	NeoMarkers
Integrin β4	3E1	1:100	Chemicon
Integrin α6	6B4	1:100	Chemicon
Collagen VII	LH7:2	1:100	NeoMarkers
Collagen IV	2311C3	1:200	Chemicon
Laminin 5	GB3	1:100	Sera-lab

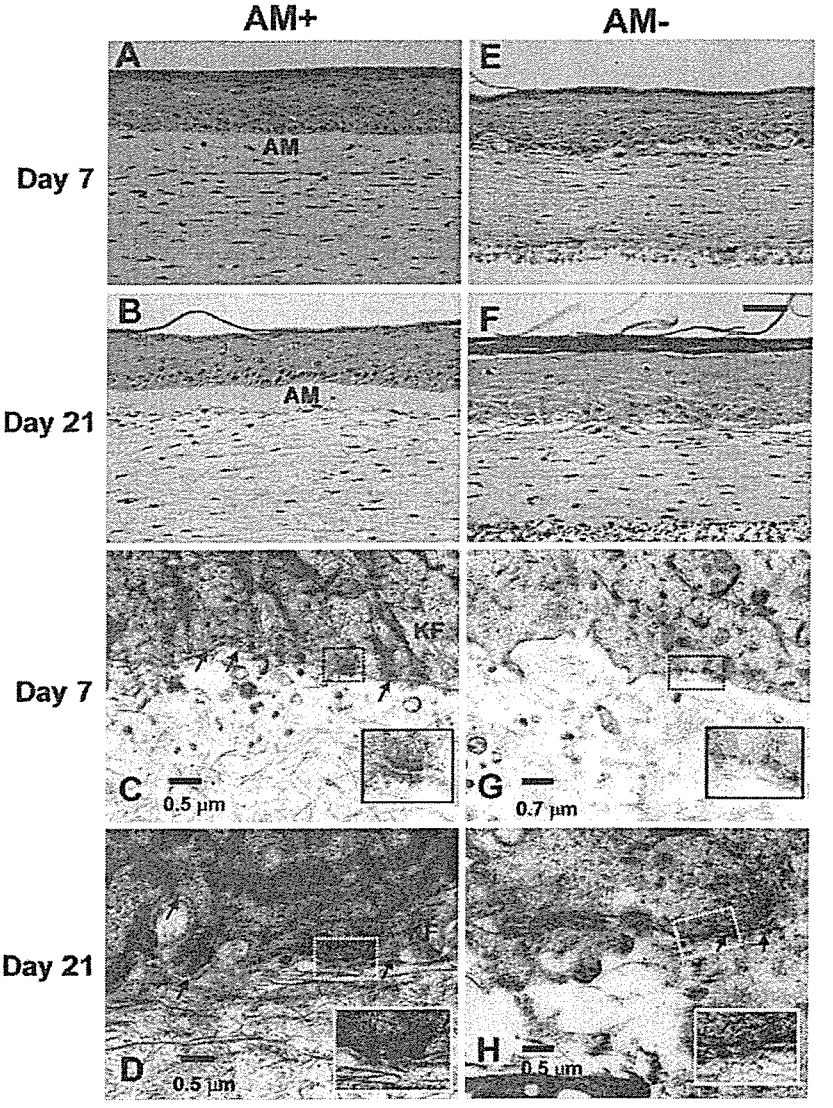

Fig. 1 Morphology of the epidermis and basement membrane (BM) in living skin-equivalent derived from amniotic membrane (AM-LSE; *AM+*) and in conventional LSE (*AM−*). Samples were harvested at days 7 (**a**, **e**, **c**, **g**) and 21 (**b**, **f**, **d**, **h**) from AM-LSE (**a**, **b**, **c**, **d**) and conventional LSE (**e**, **f**, **g**, **h**). Hematoxylin and eosin (HE) staining (**a**, **b**, **e**, **f**) showed a better-stratified epidermis with more compact, columnar basal cells in AM-LSEs. Transmission electron microscopy (**c**, **d**, **g**, **h**) revealed a more continuous lamina densa (*arrows*) and better-developed hemidesmosomes (*insets*) in the AM-LSEs than in the conventional LSEs (*KF* keratin filaments). *Bars* 50 μm (**a**, **b**, **e**, **f**), 0.5 μm (**c**, **d**, **h**), 0.7 μm (**g**)

day 21 after airlifting (Fig. 2f,p). In AM-LSE, keratin 10 expression increased with time, and by day 21, keratin 10 was distributed from the suprabasal layer to the stratum corneum, in a pattern similar to that of normal human skin (Fig. 2b,l). By contrast, keratin 10 expression decreased at day 7 and was barely observed at day 21 in the conventional LSE (Fig. 2g,q). In both LSE models, cell-cell junctions were well developed in similar patterns, as documented by the strongly expressed cell-cell junction proteins, such as E-cadherin (Fig. 2c,h,m,r), desmoglein 1 (Fig. 2d,i,n,s), and desmoglein 3 (Fig. 2e,j,o,t).

Presence of de-epithelialized AM enhances development of BM and hemidesmosomes in LSE

Types IV and VII collagen were present in de-epithelialized AM (data not shown). In the AM-LSE, immunohistochemical staining for types IV and VII collagen was seen along the epidermal-dermal junction at 7 days after airlifting (Fig. 3a,b). The type IV collagen staining was more intense at day 21 (Fig. 3k), whereas less collagen VII was observed (Fig. 3l). In conventional LSE at day 7, only small amounts of collagen IV and VII were noted along the epidermal-dermal junction (Fig. 3f,g), and although the staining increased, it still appeared minimal at day 21 (Fig. 3p,q).

The assembly of the BM was also characterized by determining the distribution of laminin 5 and its receptor, α6β4 integrin. BM normalization could be assessed by the degree to which these proteins were deposited in a polarized linear pattern at the BM zone (Andriani et al. 2003). In AM-LSE, laminin 5 was deposited linearly and was polarized along the epidermal-dermal junction at day 7 (Fig. 3c); the staining intensity had increased by day 21 (Fig. 3m). By contrast, in conventional LSE, little laminin 5 was seen at day 7 (Fig. 3h); by day 21, although more laminin 5 was expressed, its localization was discontinuous and patchy at the suprabasal layer (Fig. 3r). The receptor, α6β4 integrin, was distributed in a pattern similar to that of

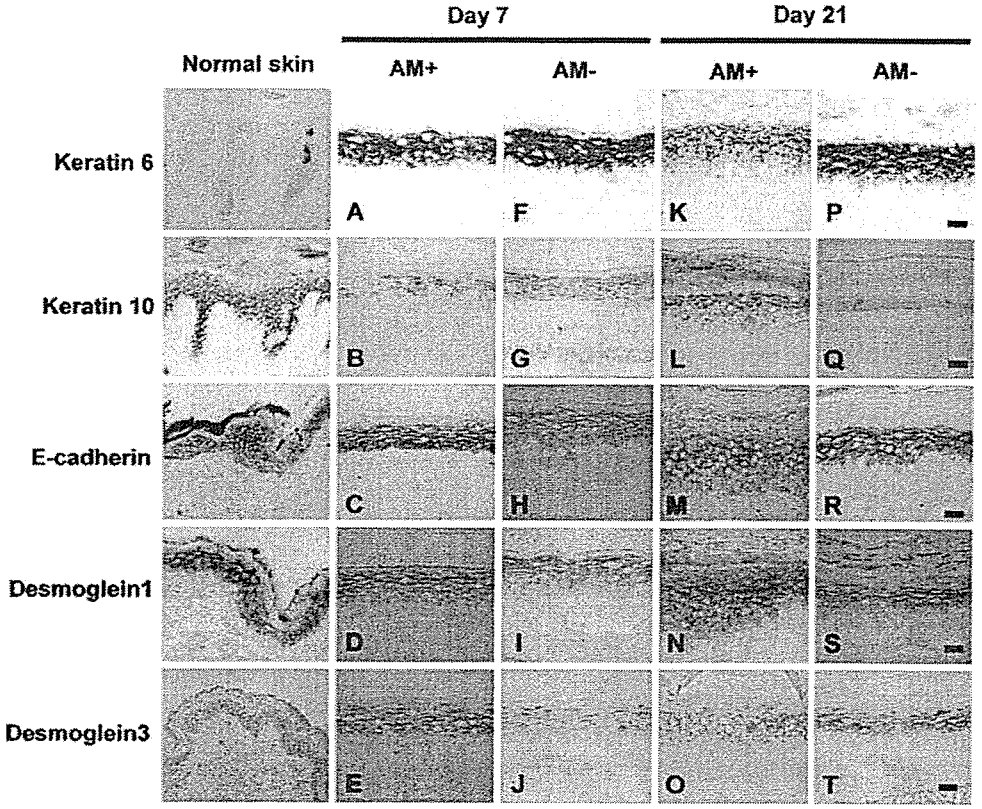

Fig. 2 Keratin and cell-cell junction protein expression in AM-LSE (*AM+*) and conventional LSE (*AM−*). Samples from days 7 (**a-j**) and 21 (**k-t**) from AM-LSEs (**a-e, e-o**) and conventional LSEs (**f-j, p-t**) were processed for immunohistochemical analysis. The expression of keratin 6 (**a, f, k, p**), keratin 10 (**b, g, l, q**), E-cadherin (**c, h, m, r**), desmoglein 1 (**d, i, n, s**), and desmoglein 3 (**e, j, o, t**) was determined by using the respective monoclonal antibodies. *Bars* 50 μm

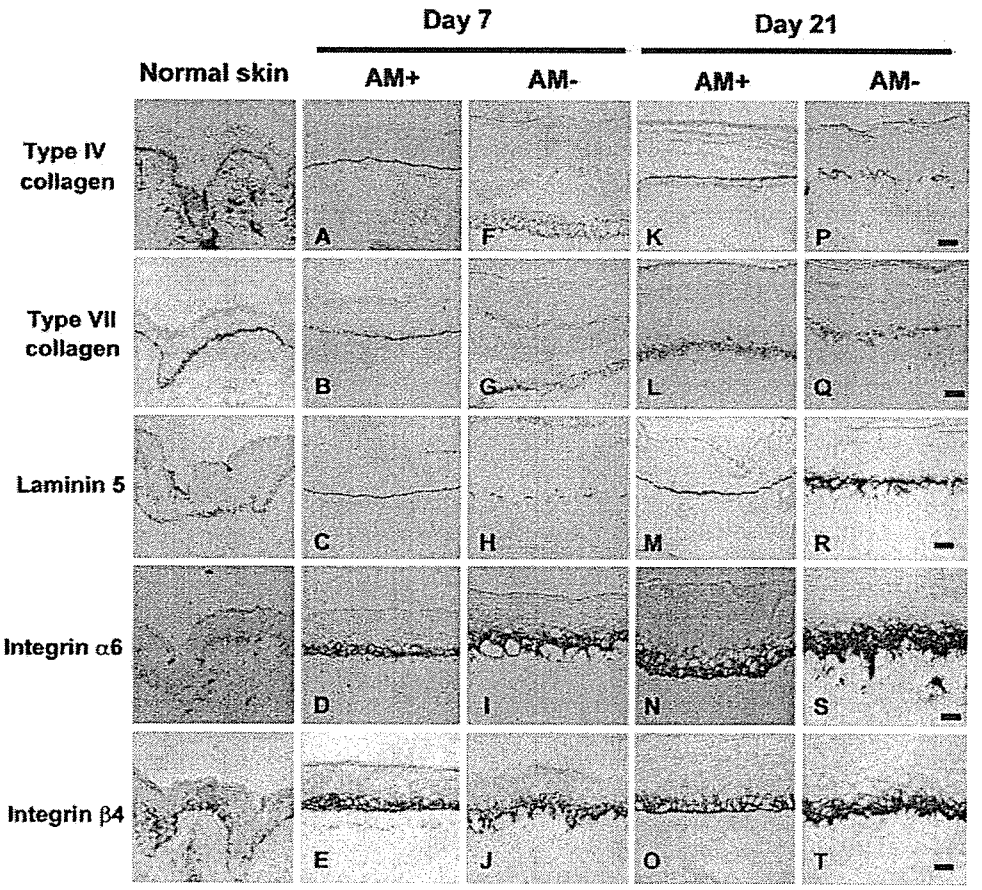

Fig. 3 Integrin and BM component expression in AM-LSE (*AM+*) and conventional LSE (*AM−*). Samples of AM-LSE (**a-e, k-o**) and conventional LSE (**f-j, p-t**) cultured for 7 (**a-j**) or 21 days (**k-t**) were stained immunohistochemically with monoclonal antibodies against type IV collagen (**a, f, k, p**), type VII collagen (**b, g, l, q**), laminin 5 (**c, h, m, r**), integrin α6 (**d, i, n, s**), and integrin β4 (**e, j, o, t**). *Bars* 50 μm